# RF FIELD EMISSION IN SUPERCONDUCTING CAVITIES

H. Padamsee, W. Hartung, R. Noer, C. Reece and Q. S. Shu

Laboratory of Nuclear Studies
Cornell University
Ithaca, NY 14853

## Introduction

Field emission is the most serious problem we face today to achieve higher gradients in superconducting accelerator cavities. Both multipacting and thermal breakdown, which used to be dominant problems of the past are well understood and under control in accelerating cavities designed for velocity of light particles. Experience at CERN, Cornell, DESY, KEK and Wuppertal show that FE is now the usual mechanism limiting achievable accelerating fields for single and multi-cell structures[1]. Experience at Argonne for structures used to accelerate heavy ions shows that field emission is also the predominant limitation after He processing to overcome low-level multipacting is complete[2]. Peak surface electric fields between 12 and 30 Mv/m and peak surface magnetic fields between 200 and 600 Oersted are achieved in full scale structures corresponding to accelerating gradients between 5 and 12 MeV/m[1]. In single cell cavities peak surface electric fields upto 60 Mv/m and magnetic fields upto 1050 Oe have been achieved[3]. When compared with the 200 Mv/m dc surface fields achieved with $cm^2$ size, clean, heat-treated Nb surfaces[4], and with the 2400 Oe theoretical rf critical magnetic field capability of Nb[5], it is clear that there remains much room for improvement with Nb cavities.

## A high speed/superfluid FE temperature mapping system

Use of a temperature mapping technique to locate and analyze emission sources has been well established. Since the last workshop, two major advances have taken place in this technique: a) operation in superfluid He and b) reduction of the time to acquire a map at a single field level from 30 minutes to 15 seconds[7].

For high field studies, operation in superfluid He is necessary, especially for frequencies > 500 Mhz. In subcooled He temperature diagnostics, the low heat transfer coefficient of subcooled He as well as the higher operating temperatue (2.2 K) can force the rf surface temperature to increase unstably at high fields due to BCS losses[8]. As an added benefit, heat flow calculations and thermometer response calibration experiments show that the spatial resolution of superfluid thermometry is increased by a factor of 2.5 over subcooled He thermometry[9].

To obtain a map in a few seconds, the outer wall of the cavity is covered with a large number of thermometers at fixed locations rather than mechanically moving a smaller array over the surface. With improved acquisition speed, it is now possible to study local heating as a detail function of field level and to study the time dependent behavior of emitter heating.

At Cornell, we are using this system in conjunction with single cell 1500 Mhz cavities to study the statistics and properties of emitters as we vary the surface treatment (See Fig. 1). We have started to explore heat treatment and are studying He processing. A similar system is under preparation for 3000 Mhz cavities at the U. of Wuppertal[10]. This system also includes an X-ray detector array placed adjacent to the cavity[3].

Details of the fast/superfluid T-mapping system have already been described in refs. 7. We will concentrate in this paper on some of the salient results obtained with the system. Much data still remains to be analyzed to extract information on number density of emitters, their $\beta$ and emissive area values.

A method to determine $\beta$ values for individual emission sites has been worked out. In the past, the detailed shape of the T-map at a fixed azimuth and fixed field was analyzed to extract the $\beta$ value[6]. This method worked well at 500 Mhz for $E_p$
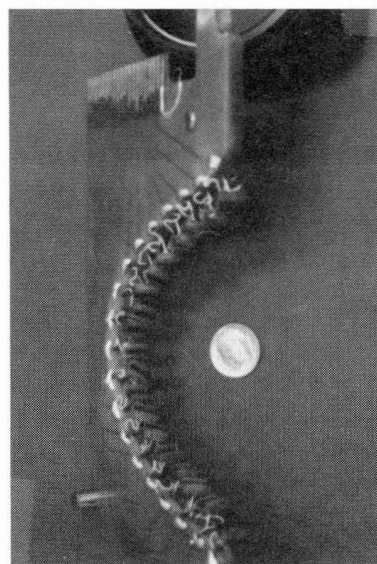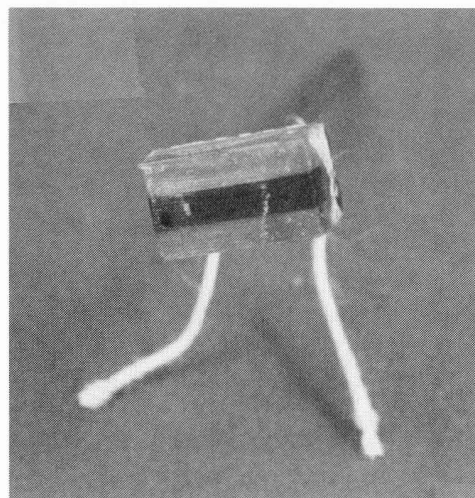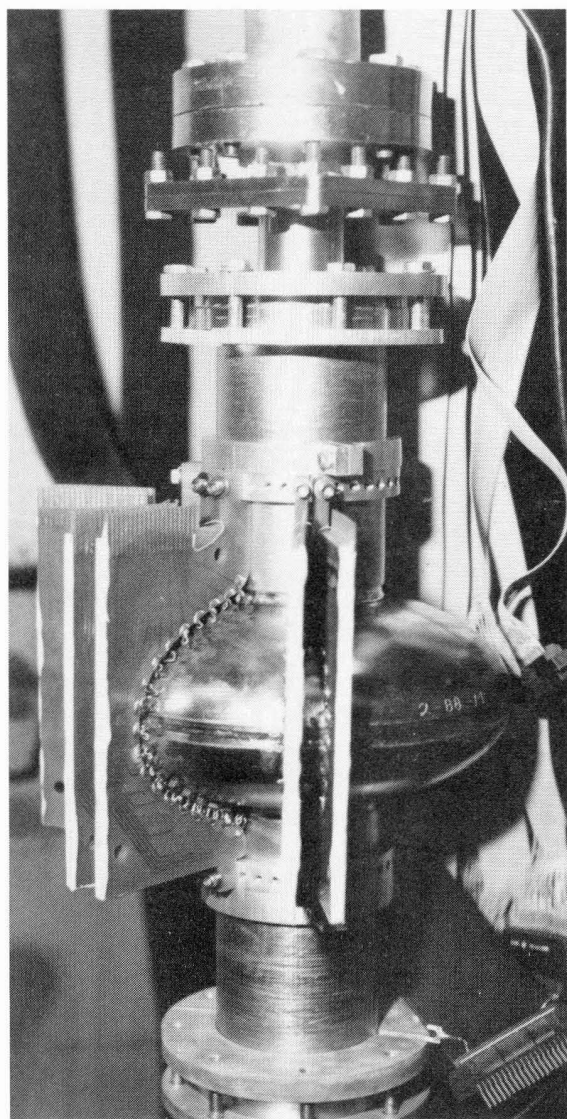
Fig. 1 High speed superfluid temperature mapping system for a 1-cell 1500 Mhz cavity. Printed circuit boards bearing 19 thermometers each are placed 10° apart around cavity outer wall.

SRF87C03

between 10 - 20 Mv/m because changes in $\beta$ influence the shape of T-maps sufficiently to extract $\beta$. At 1500 Mhz, our calculations show that between 15 - 30 Mv/m, $\beta$ does not affect the shape significantly. Instead we use our capability for rapid T-maps to make several T-maps at increasing field levels and from these to determine $\beta$ from the slope of the Fowler-Nordheim plot of $\Delta T_{peak}/E^2$ vs. $1/E$. This technique for determining $\beta$ is confirmed by adopting an analogous procedure using calculated T-maps. To obtain a "calculated T-map", we first calculate field emitted electron trajectories (Fig 2a), following similar previous computational efforts. By smearing the power deposited by the impacting electrons to simulate heat flow through the Nb wall, we then calculate the corresponding T-map for an emitter with a chosen $\beta$ at a chosen location. The procedure is repeated for several field levels and the corresponding calculated T-maps shown in Fig. 2b. A F-N plot of $\Delta T_{peak}/E^2$ vs. $1/E$ from these maps is shown in the companion Fig 2c. A $\beta$ value is determined from this slope and found to be 20% lower than the starting $\beta$. The procedure has been repeated for several fields between 15 -30 Mv/m, always showing a linear F-N behaviour and a consistent 15 - 25% underestimate of $\beta$. Therefore $\beta$ values from experimental T-maps are uniformly scaled up by 20%. Individual emitter T-maps at particular field levels can also be fit in detail to obtain $\beta$, but this procedure is more painstaking.

Another important consideration enters into the analysis for $\beta$ from experimental T-maps. To separate heating produced by impacting electrons from heating by other sources (eg. dielectric or resistive losses) we plot $\Delta T$ vs. $E^2$ over a large field range as in Fig. 3a. At low fields we usually observe a linear behavior such that $\Delta T$ goes to zero at zero E. When FE starts, we get departures from a simple linearity. The true FE heating $\Delta T$ is obtained by subtracting out the linear component due to other losses. This subtraction influences the determination of $\beta$, especially for emission that is weak compared to other heating. A F-N plot for the FE component of $\Delta T$ is shown in Fig 3b, from which a $\beta$ value of $325 \times 1.2 = 390$ is determined. In cases where He processing reduces emission, we find the heating to return to the linear behavior as shown in Fig. 4, justifying our procedure for linearly extrapolating the other losses into the non-linear FE emission regime. $E^2$ losses also influence the shape of the FE induced heating profile, so that a detailed comparison of the shape with trajectory calculations needs a point by point $E^2$ subtraction.

SRF87C03

(a)

$E_{PK} = 23.7$ Mv/m

Y AXIS (m)

Z AXIS (m)

(b)

(C)

β 500.0
σ 0.70

$E_{PK} = 23.7$ Mv/m

22.5 Mv/m

21.1 Mv/m

19.7 Mv/m

18.2 Mv/m

TEMPERATURE CHANGE [mK] (×10⁵)

S LOWER [cm]

β 500.0
FITβ 376.1      ± 4.9
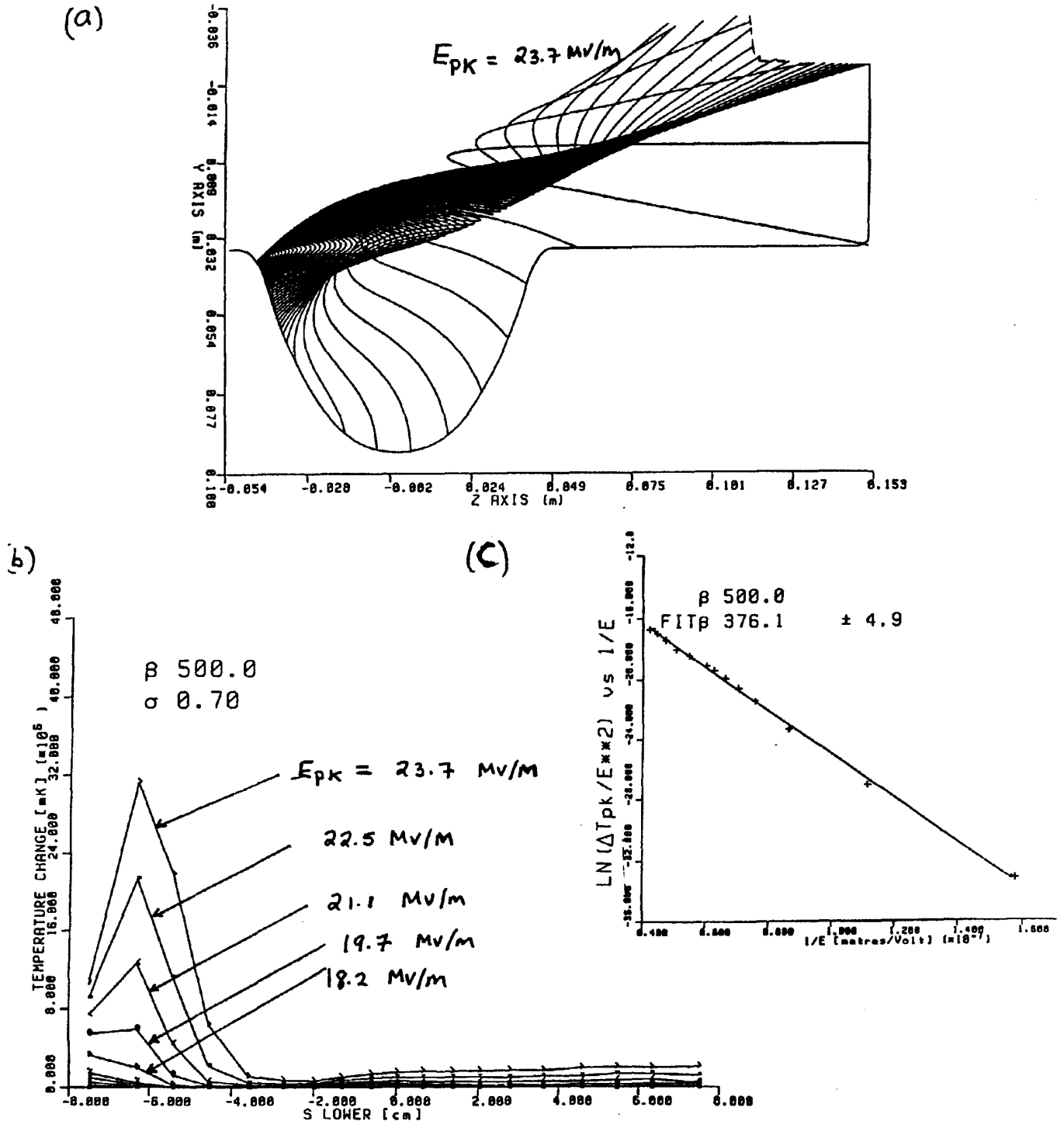
LN (ΔTpk/E**2) vs 1/E

1/E [metres/Volt] (×10⁻⁷)

Fig. 2 (a) Trajectories of field emitted electrons emanating during one rf period from a field emission source on the cavity surface located near the maximum electric field. The peak surface field for this calculation is 23.7 Mv/m
(b) Calculated heating profiles for various field levels at a fixed azimuth due to impact of field emitted electrons. A β value of 500 is assumed for the emitter.
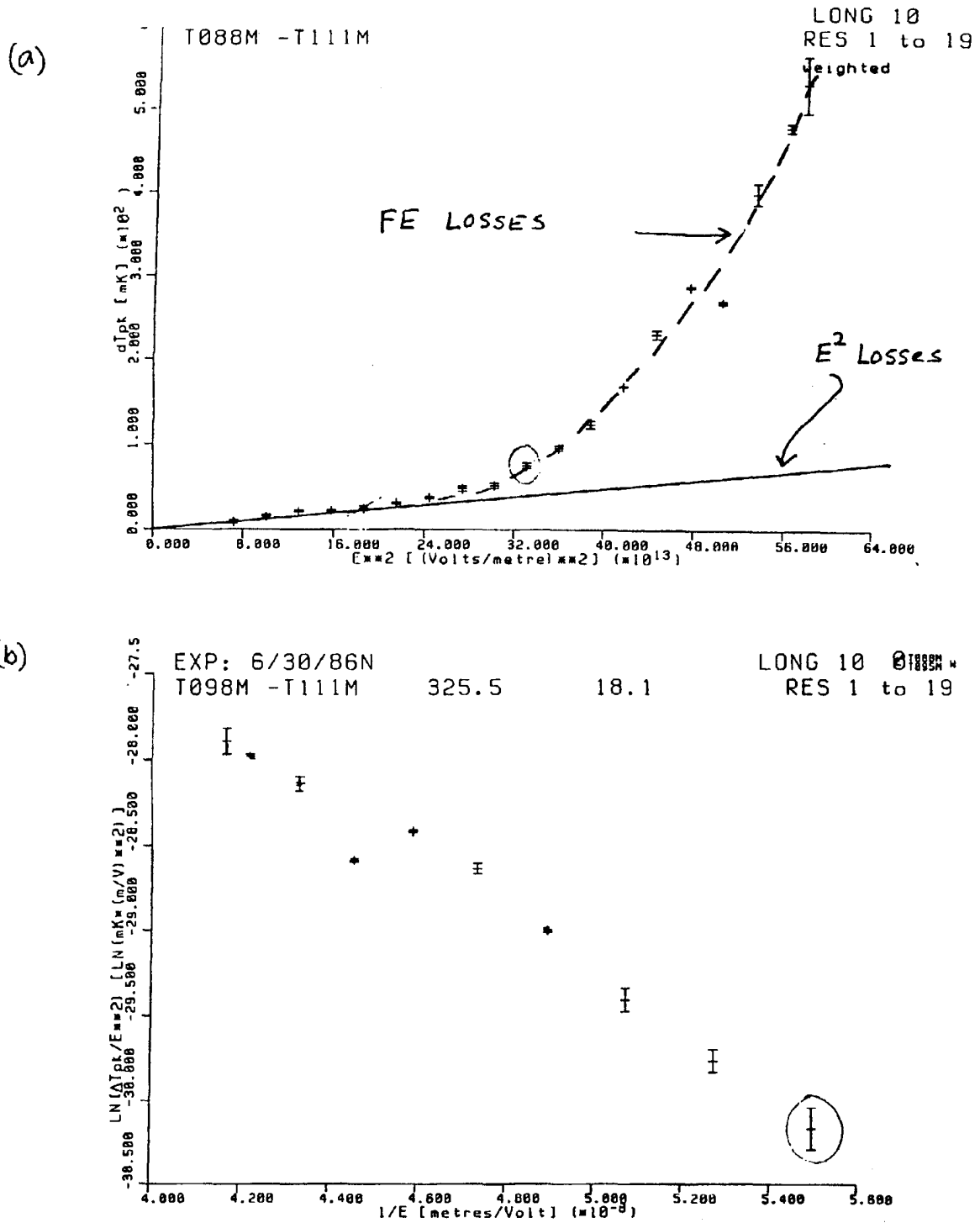(c) Fowler Nordheim plot of the calculated peak temperature increment ΔT. β value determined from the slope is 376.

Fig. 3 Maximum temperature increment at a particular azimuth as a function of $E^2$. Two components of heating, one due to field emission (FE) and the second due to other losses are visible in (a). The field emission component increases non-linearly above 15.5 Mv/m. (b) Fowler-Nordheim plot of FE component for heating at the same location. The slope gives a $\beta$ value of 325x1.2 (see text).
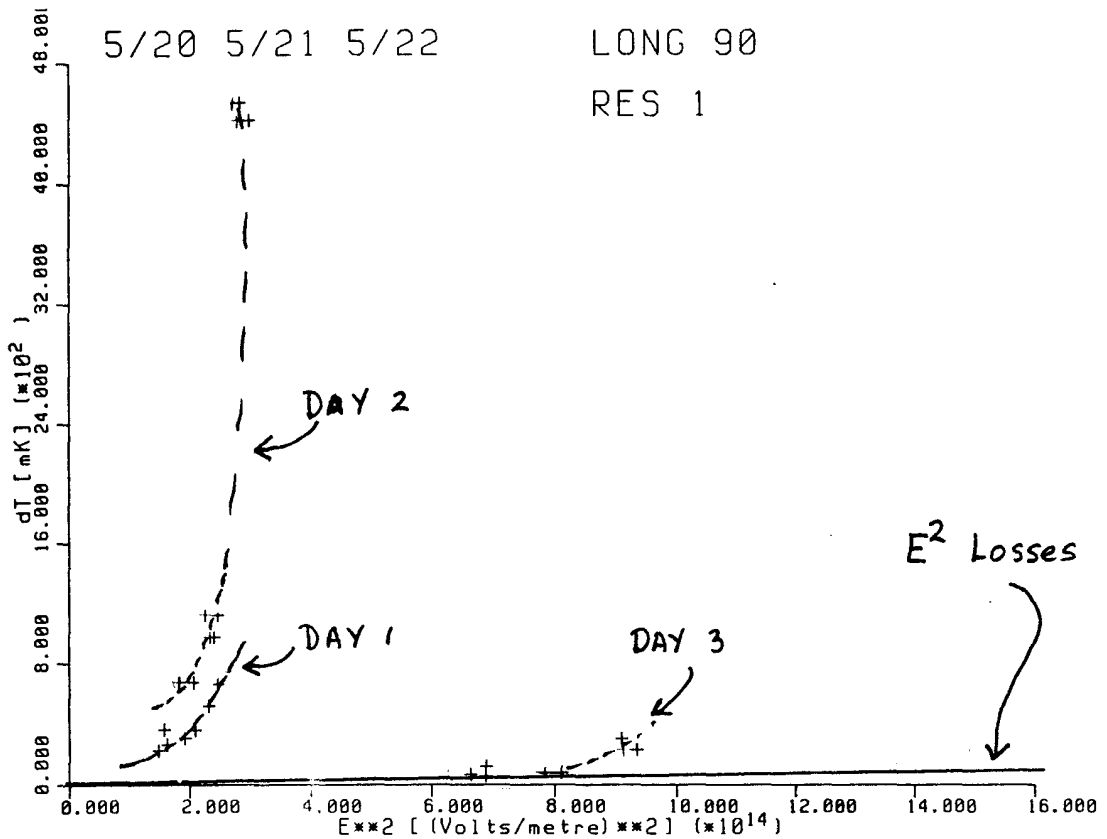
SRF87C03

Fig. 4 Heating due to field emission and other losses at a particular location during various phases of He processing. Note that the FE heating returns to a $E^2$ behavior when the processing is successful. This observation is the basis of subtracting $E^2$ losses to obtain the FE heating component alone when both are present.

## Emitter Switching

The most serious problem that we have encountered with FE in our cavities is the frequent switching of sites to highly emissive states. In some instances, the switching manifests itself as an abrupt increase in heating as the field level is increased. One example is shown in Fig. 5. In many cases, however, the switching is accompanied by a spontaneous decrease in the cavity field level. Even though the field decrease does reduce emission from the swtiched site, the emission continues at a level higher than before the switch. β values are observed to be enhanced substantially. We refer to this phenomena as state II . Before this severe switch sets in, field emission is labelled as pertaining to state I. When state II sets in, a correlated jump in the current collected by the rf antenna is also observed, along with increased heating at specific locations. One example of state II is given in refs. 7. Here the time dependence of FE induced heating is shown at the onset of state II. Another example is discussed in this report in Fig. 6. Comparison of a state I with a state II map at about the same field level shows the emergence of at least two stronger sites, one at the top iris near 230° and another at the bottom iris near 90°. A superposition of the temperature profiles at fixed latitudes, both top and bottom, shows in detail the emergence of the state II sites (Fig. 6b). As will be discussed below, heat treated cavities are also observed subject to state II. Fortunately, He processing does have a beneficial effect on emission in state II.
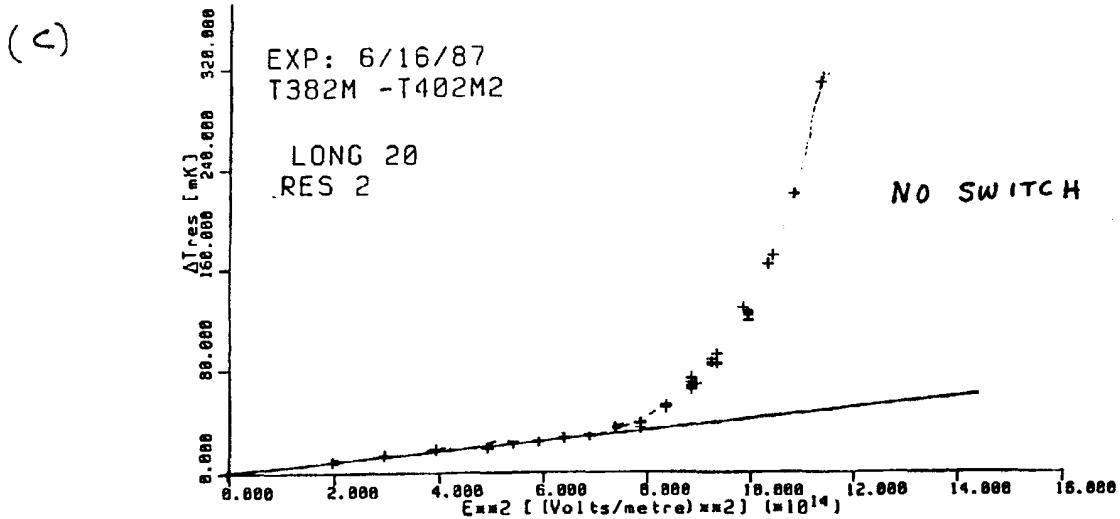
(a)

$E_{pk} = 31.5 \text{ Mv/m}$

Normal FE (C)

MINOR SWITCH (b)

(b)

EXP: 6/16/87
T382M -T402M2

LONG 12C
.RES 19

MINOR SWITCH

ΔTres [mK] (×10²)

E**2 [ (Volts/metre)**2 ] (×10¹⁴)

(c)

EXP: 6/16/87
T382M -T402M2

LONG 20
.RES 2
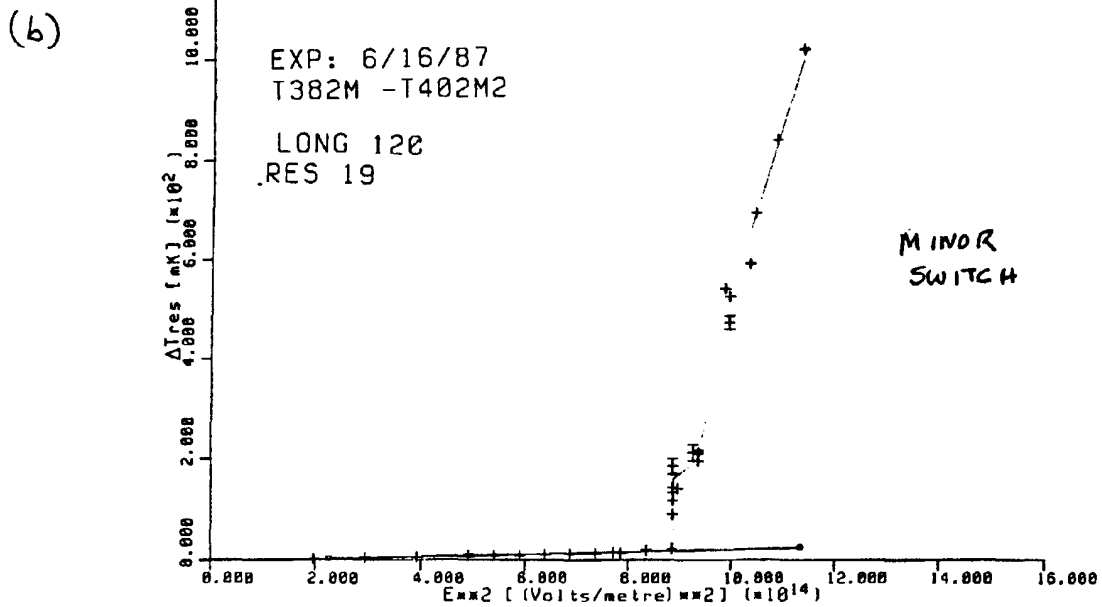
NO SWITCH

ΔTres [mK]

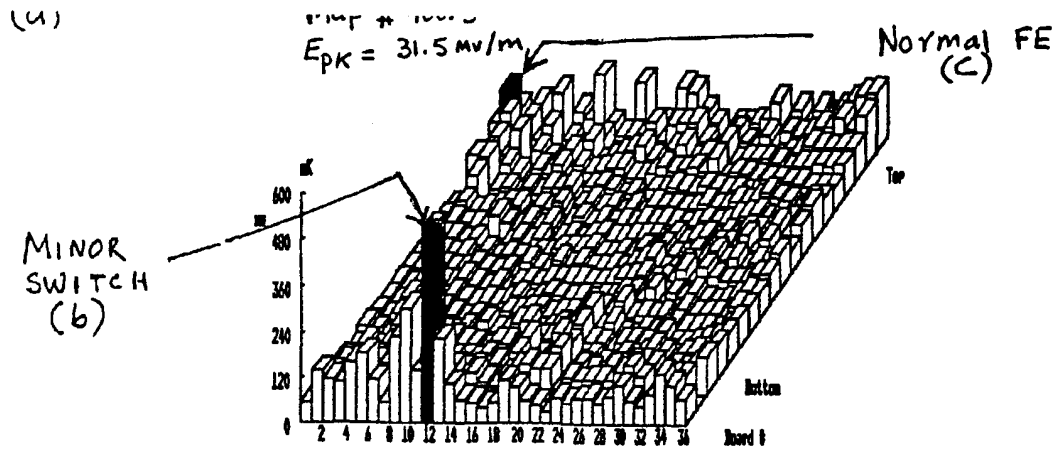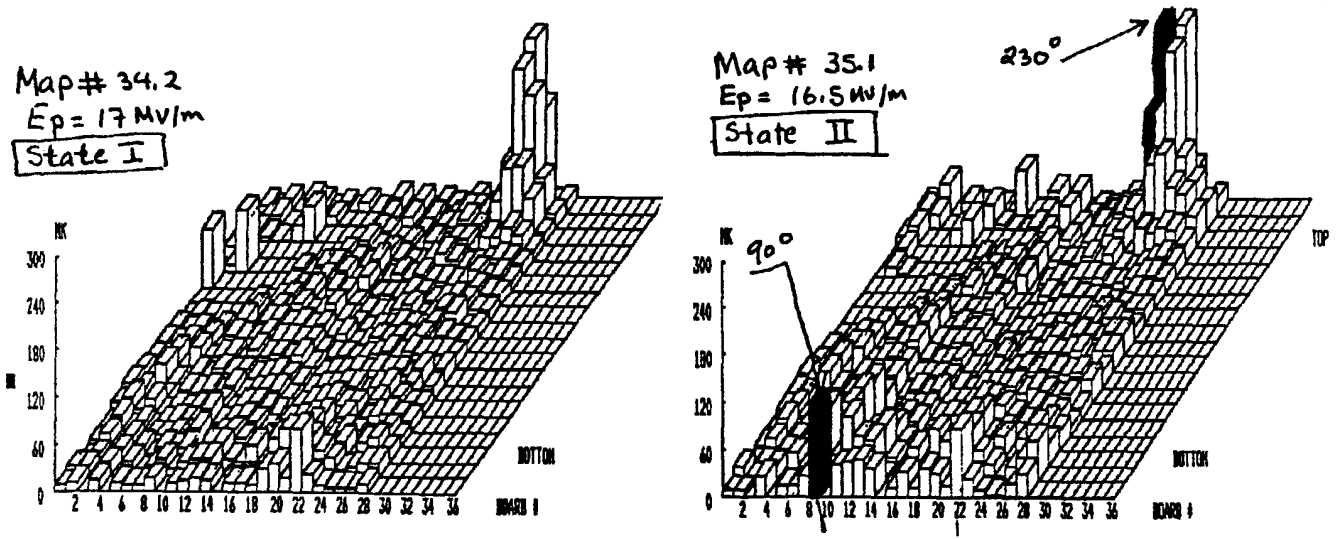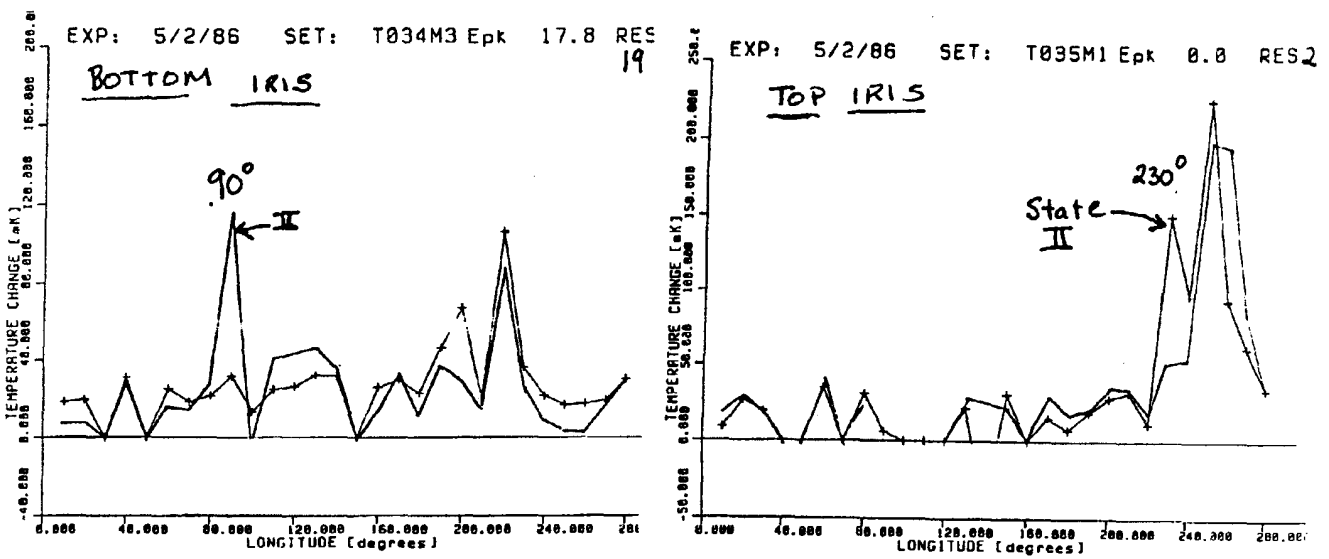E**2 [ (Volts/metre)**2 ] (×10¹⁴)

Fig. 5 (a) Temperature map at 31.5 Mv/m after a minor switch. The evolution of emission at the switched site is shown in (b) for increasing E, the switch is apparent near 30 Mv/m. For comparison (c) shows the evolution of heating at a regular site where no switching is observed.

SRF87C03

(a)



(b)

Fig. 6 (a) Comparision of temperature maps at before and after a major switch. Two sites at 90° and 230° that switch are shaded. Cross-sections of the maps at a fixed latitude near the top and bottom irises are shown in (b). The appearance of substantial heating after the switch is evident at 90° and 230°.

## Influence of Heat Treatment on FE

One of the most interesting questions regarding FE in rf cavities is whether heat treatment of cavities reduces emission and permits higher fields, as suggested by the U. of Geneva dc FE measurements.[4] Recent tests on high purity Nb 3 Ghz cavities show that the field level ($E_p$) for the onset of FE ranged from 1.0 to 21.0 Mv/m for chemically prepared surfaces, whereas for a heat treated surface which had been subsequently handled in a dust-free manner, the onset values ranged from 6.5 to 42 Mv/m. The highest field reached after rf and He processing was 16.3 to 52.5 Mv/m for chemically treated surfaces and from 44.6 to 58.9 for heated surfaces followed by dust-free handling. These results are just above the threshold of statistical significance for demonstrating the beneficial effect of heat treatment.[3]

A comparison of emission maps between a heated and chemically treated surface helps to strengthen this trend. Fig 7a. compares a temperature map of a 1.5 Ghz chemically treated cavity (#LE1-20) at the highest field level reachable after processing, 24 Mv/m, with the map (Fig 7b) at the same field level on the first test on the same cavity after heat treatment at 1200 C. There is a substantial reduction in the number and severity of emisssion sites. Only one site is clearly identifiable after heating, whereas 8 sites have been clearly identified for the chemical treated surface. Their β values and maximum $\Delta T$ values are listed in Table 1. Note that for the chemically prepared surface test, only 78% of the total cavity area was covered because in the early stages of development of the new diagnostic system, the complete set of thermometers were not available.

Above this field level (24 Mv/m), state II emission increased the severity of the loading drastically in both cases. However for the fired cavity it was possible to use He processing to raise the field level to 31.8 Mv/m, when the map shown in Fig. 7c was taken. We are still in the process of analyzing the number and properties of the emitters present at this level, but the map clearly shows that in State I the total emission heating is still far below that visible if Fig. a (State I) corresponding to the chemically prepared surface.

## Table 1

Emitter properties at 24 Mv/m, chemically prepared surface. The fit β values should be increased by 20% as discussed in the text.

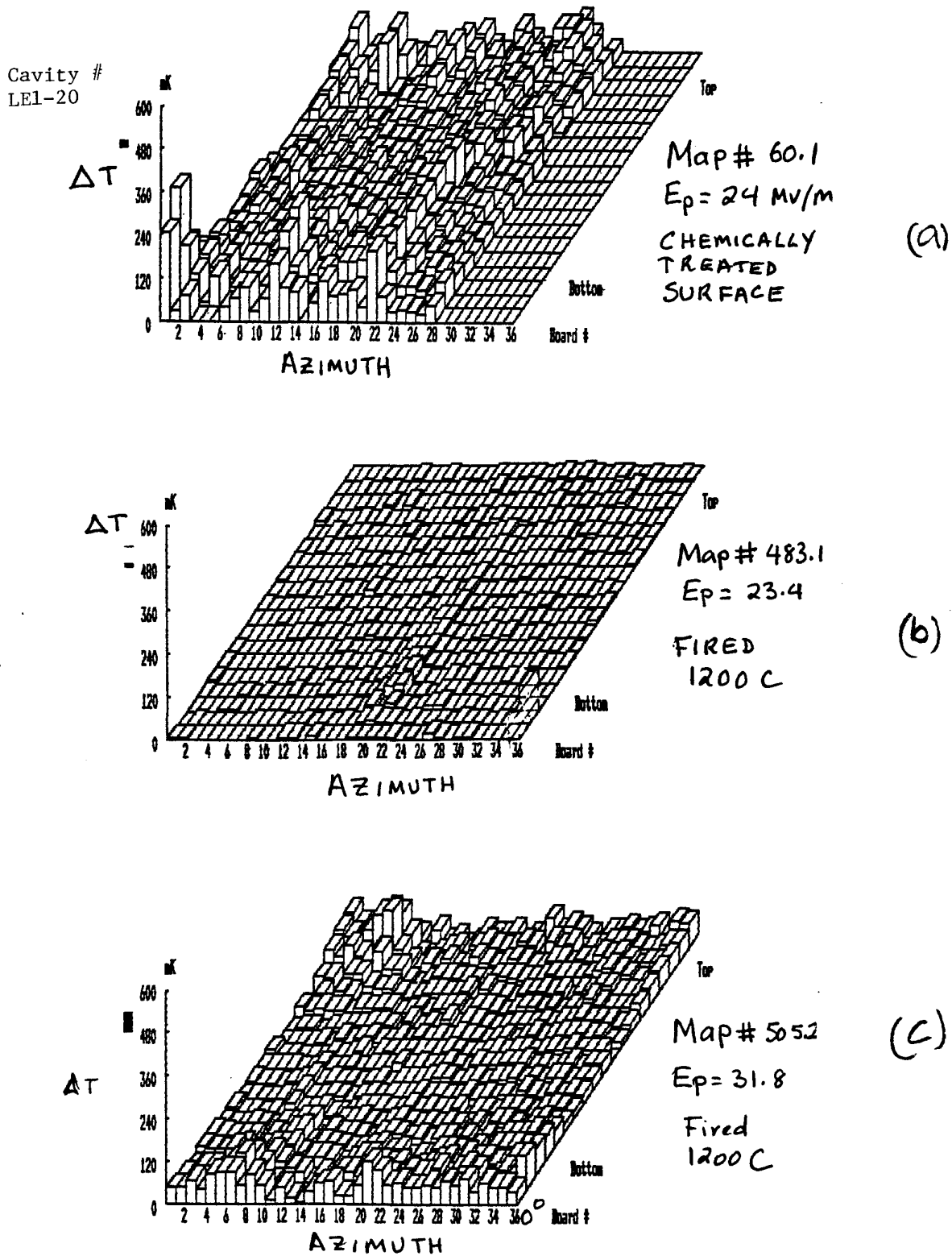| Location | Fit β (mK) | ~ $\Delta T$ (max, FE) | Comments |
|---|---|---|---|
| 10°, bottom | 427 ± 26 | 450 | |
| 30° | | | Rf Processed |
| 90°, bottom | 1140± 200 | 80 | |
| 120°, " | 477 ± 100 | 200 | |
| 200° " | 685 ± 90 | 220 | |
| 220° " | ? | | $E^2$ component very large |
| 200° top | 234± 30 | 250 | |
| 250° " | 468± 116 | 160 | |
| 260° " | 372± 48 | 160 | |

Fig. 7 (a) Temperature map at 24 Mv/m for a chemically prepared surface for cavity LE1-20, after He processing to reach the emission limited field level. Detail examination of this map reveals about 8 emitters ($\beta$ values are given in Table 1). Only 28 out of 36 boards were available in the early stage of the thermometry development project when this experiment was performed. (b) Temperature map of the same cavity at a comparable field level after heating at 1200 C. Note the significant reduction in emission in comparison, no He processing. (c) Map obtained near the highest field level 31.8 Mv/m, after He processing.

261

SRF87C03

Another set of comparisons between heated (1100C) and chemically treated surfaces on a separate cavity, #LE1-21, is shown in Fig 8. For the chemically treated case, the highest field we were able to reach was 21 MV/m, limited by heavy emission in state II as compared to a maximum field of 34.3 Mv/m for the heated case, also limited by state II. In both cases He processing was also applied. The first map (a) in Fig 8. was taken near the highest field (18.3 Mv/m) we were able to reach in State I for the chemically prepared case, and this should be compared with maps taken in state I for the heated case at 19.8 (Fig. 8b), 24.3(Fig. 8c) and 31.5 (Fig. 8d) Mv/m each. At 31.5 Mv/m, the field emission loading in the heated case is finally comparable to the loading at 18.3 Mv/m, as judged by the integrated area under the temperature maps. At 34.3 Mv/m , the total area in the heated case increases by another factor of 3. A count and analysis of emitter properties for these tests is in progress.
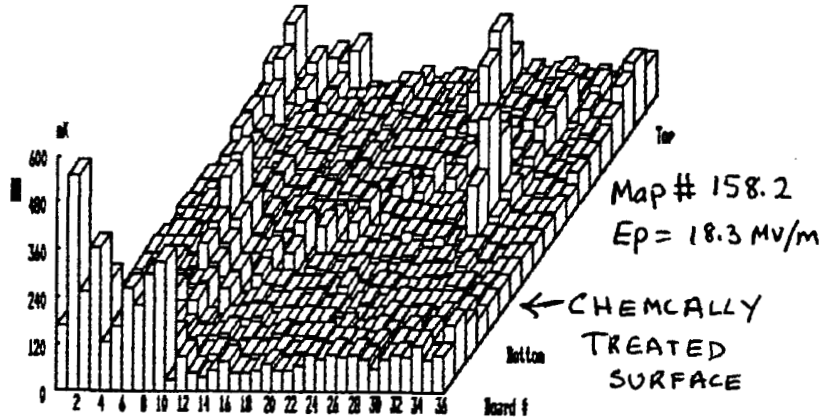
Both cavities therefore show improvement in FE loading when viewed in terms of the maximum achievable fields or by comparing the temperature maps. The disappointing feature, however, is the persistence of state II, even after heat treatment, continuing the need to He process to overcome this serious problem.
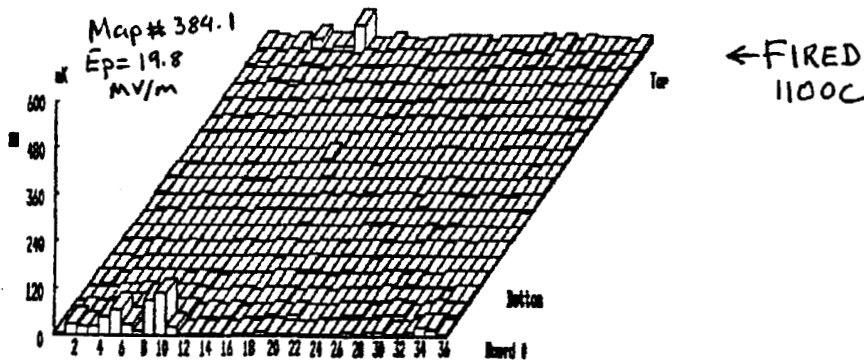
### Effect of Exposure to Dust-Free Air

Another interesting question is how the emission properties of a surface which can reach in excess of 30 Mv/m are affected after a controlled exposure to 1 atm. with filtered dust-free air. We tested this question using cavity LE1-21 which was fired (1100C) and He processed to exceed 30 Mv/m. Fig 9. compares State I T-maps before(a) and after(b) exposure at a field level of 32 Mv/m. The maps show that the exposure did not inundate the cavity with new sources. However, emission activity previously observed in certain areas had increased. The integrated area under the maps showed a 50% increase with exposure . As an example, Fig.9 shows in more detail the effect at locations 60° (c vs. d) and 100° (e vs. f). Here $\Delta T$ is plotted for increasing field levels. After exposure, increased FE heating is clearly visible above the linear $E^2$ losses. These results suggest that the dominant sources of FE are not in clean air, but that existing emission sites may be influenced by exposure to gases.

SRF87C03

CAVITY #
LE1-21

(a)

Map # 158.2
Ep= 18.3 Mv/m
←CHEMICALLY
TREATED
SURFACE

Map # 384.1
Ep= 19.8
Mv/m

(b)

←FIRED
1100C

Map # 388.1
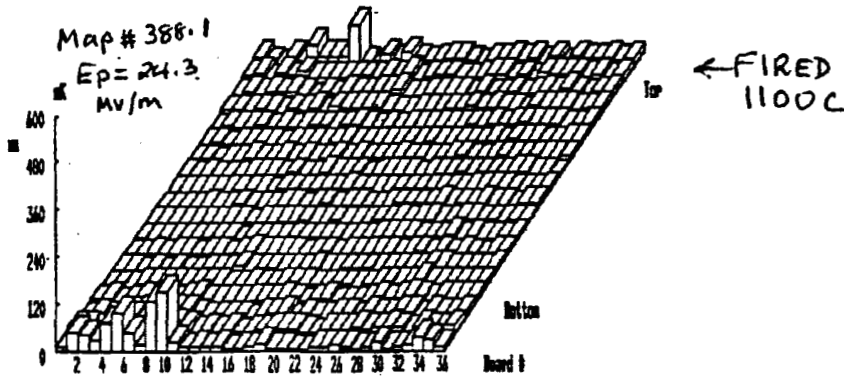Ep= 24.3
Mv/m

(c)

←FIRED
1100C

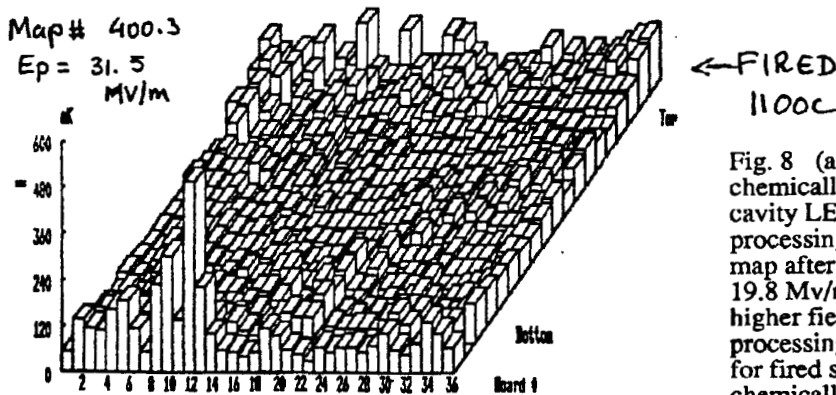Map# 400.3
Ep= 31.5
Mv/m

(d)

←FIRED
1100C

Fig. 8 (a) Temperature map of
chemically prepared surface for
cavity LE1-21 at 18.3 Mv/m after He
processing applied. (b) Same cavity
map after heat treatment at 1100 C at
19.8 Mv/m. (c) and (d): Maps at
higher field levels after He
processing. At 31.5 Mv/m emission
for fired surface is comparable to
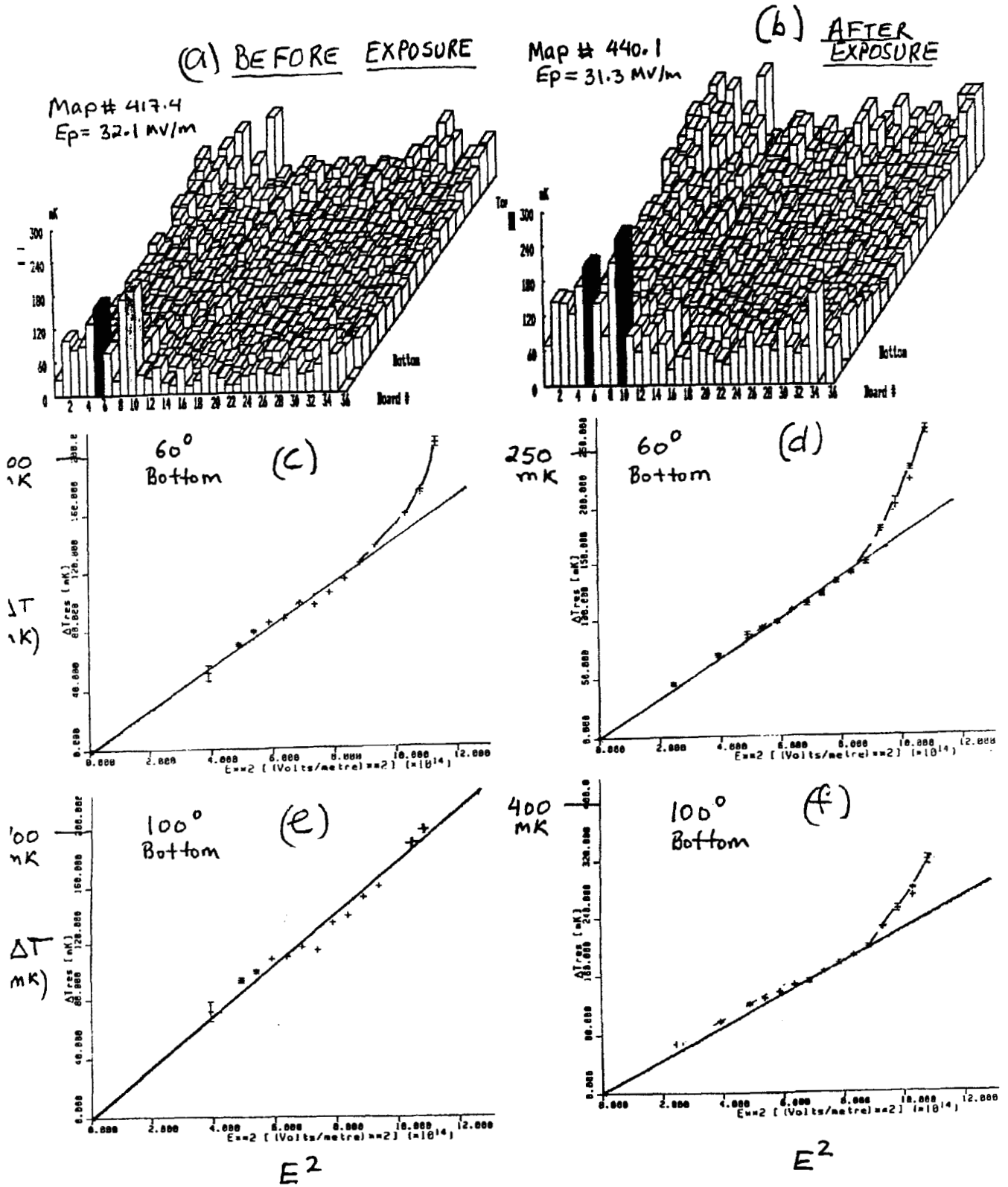chemically prepared surface at 18.3
Mv/m.

Fig. 9 Comparison of maps before and after exposure to dust-free air at 32 Mv/m. Emission at some sites is enhanced, as shown for example at 60° and 100° by comparing (c) with (d) and (e) with (f).

## He and Rf Processing

It has been well established by other workers that He processing is an effective remedy against FE[11]. Using a sequence of temperature maps during processsing it has also been shown that individual emitters can be suppressed[6]. We have confirmed this effect on several tests, one example is discussed here in detail. Cavity LE1-21 showed heavy state II emission at 16.6 Mv/m during the first test after firing as shown in map a of Fig. 10. Immediately after admitting He the first map (b) showed the sudden loss of several major emission areas, dropping the integrated power by a factor of 5. Further increase in field level increased the emission at one of the dominant sites, until it also was eliminated, allowing the field level to jump up to 21.5 Mv/m (map e ) when the integral power dropped by a factor of 2.5. As the field level was increased new emitters were visible (map f ), but these too were successfully processed until 30.8 Mv/m. After the processing it was found that 31 Mv/m could be achieved continuously in State I.

The detailed heating ($\Delta$T) at five of the processed sites is plotted as a function of $E^2$ in Fig. 11 before and after He processing. Processing of sites located at 20°, 40°, 90°, 180°, and 320° is presented. Before the He was admitted all the sites were clearly emitting between 12 and 16 Mv/m. Immediately after He admission there was a substantial drop in the emission from 4 out of 5 sites, but one site (90°) increased. On further processing between 15 and 16 Mv/m, this emitter too processed away accompanied by an abrupt increase in field level to above 20 Mv/m. As this emittter processed, the emission increased substantially before dropping abruptly. Between 26 and 30 Mv/m, emission at three of locations shown re-intensified and then processed away. It is not clear whether new emitters at the same locations were visible because of the higher field or whether the older emitters were active again.

To summarize, He processing reduces emission at most sites, but occasionally, admission of He can enhance emission at some sites. Perhaps this is due to contaminants in the He condensing on existing sites. Following this possibility, we are about to embark upon special efforts to clean the He gas before admission into the cavity.

RF processing has not been found to be as beneficial as He processing, in agreement with similar observations from other workers. One example of rf processing is described in Fig. 10. Emission is reduced at this emitter but not eliminated as seen when the field level is raised.

## Reduction of FE on Temperature Cycling

Very often we have observed that after rf or He processing under heavy FE loading, cycling to room temperature increases the onset field for the appearance of State II by about 10%. For example after He processing to achieve 31 Mv/m in state II, we cycled to room temperature. On cooling down we were able to achieve a comparably high field but in state I. Fig. compares the emission heating at the same field level before and after the cycling. Futher testing showed that a maximum field of 34 Mv/m could be reached in state I for this follow-up test. These results suggest that heavy processing somehow conditions a site and that further room temperature heating assists the process. When put together with the observations that admission of He can occasionally enhance emission at specific sites, and that controlled exposure of a cavity to dust-free air promotes emission, the importance of the role of condensed gases in the emission process is re-inforced.
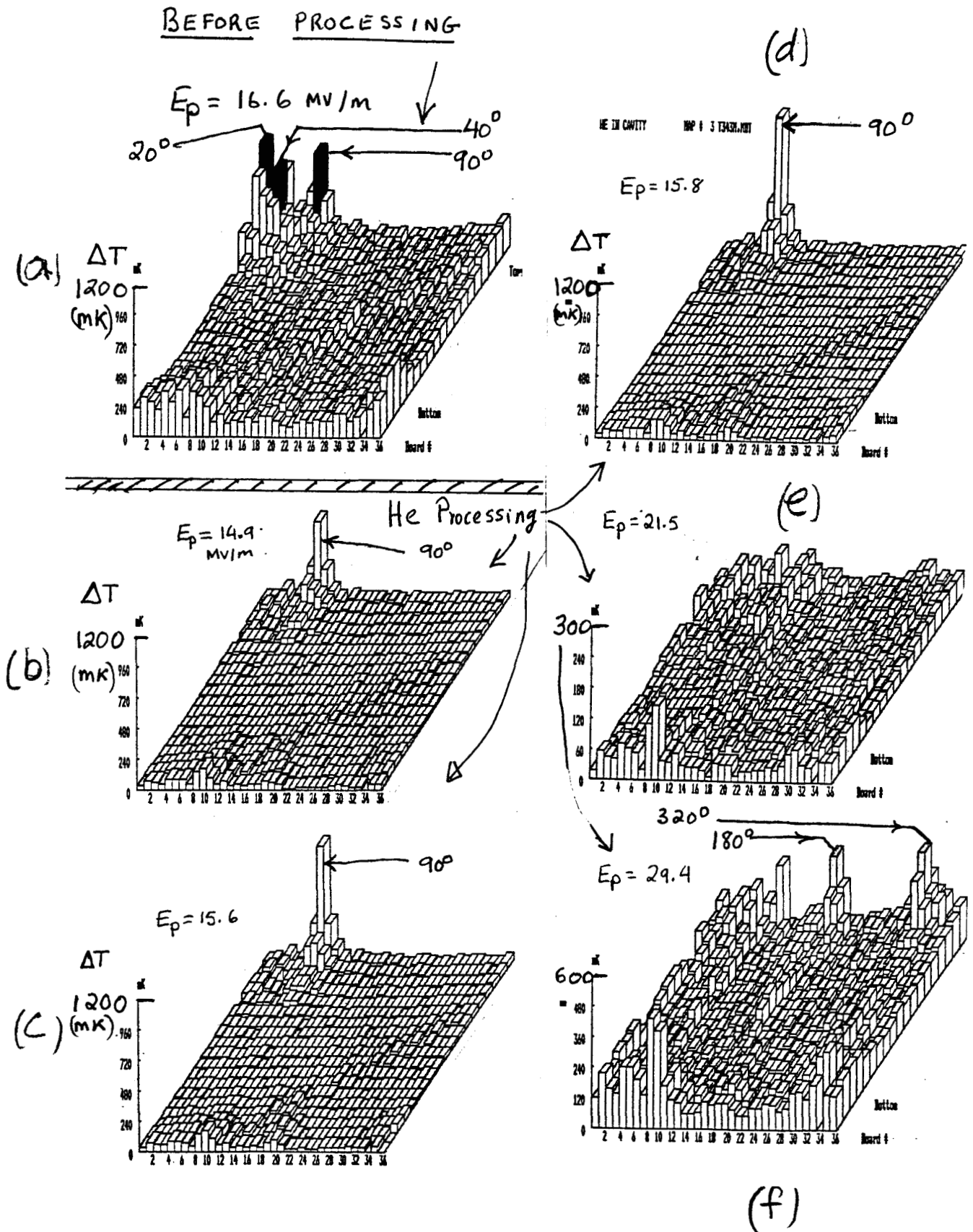
BEFORE PROCESSING

(d)

$E_p = 16.6$ MV/m

$20°$  $40°$  $90°$

(a) $\Delta T$ 1200 (mK)

HE IN CAVITY    MAP # 3 T3434.MDT

$E_p = 15.8$    $90°$

$\Delta T$ 1200 (mK)

He Processing

$E_p = 14.9$ MV/m    $90°$

$E_p = 21.5$    (e)

(b) $\Delta T$ 1200 (mK)

$300$

$E_p = 15.6$    $90°$

$320°$    $180°$

$E_p = 29.4$

(C) $\Delta T$ 1200 (mK)

$600$

(f)

Fig. 10  (a) Map showing heavy emission in State II at 16.6 Mv/m just before the start of He processing. (b)-> (e): Progress in He processing in state II.  Note change of ΔT scale in (e) when emitter at 90° is successfully processed.
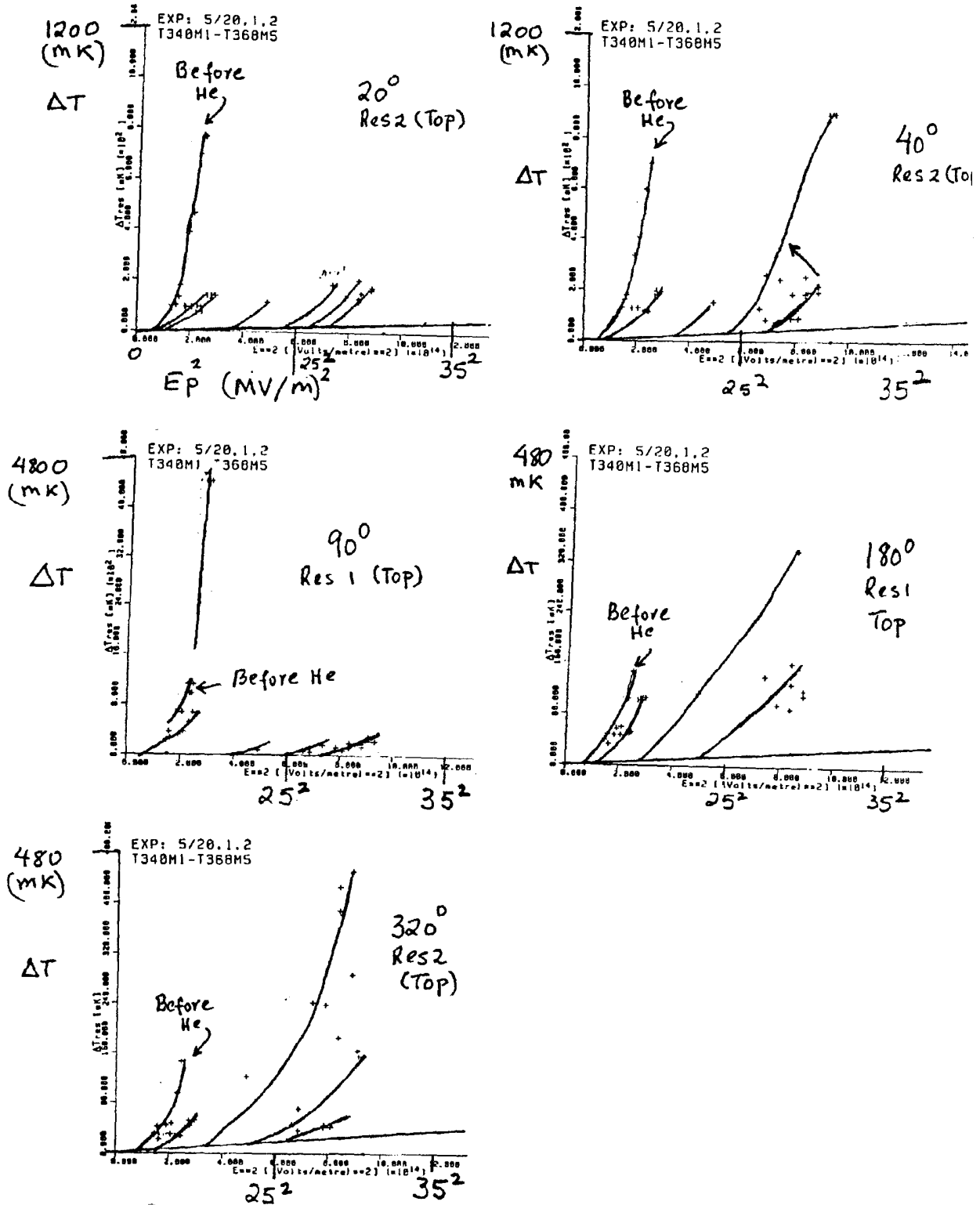
SRF87C03

Fig. 11  Detail behavior at various field levels for individual emitters that successfully processed as visible in Fig. 9.  In 4 out of 5 cases shown emission decreased on first admission of He.  But at 90°, emssion first increased substantially before successful reduction.
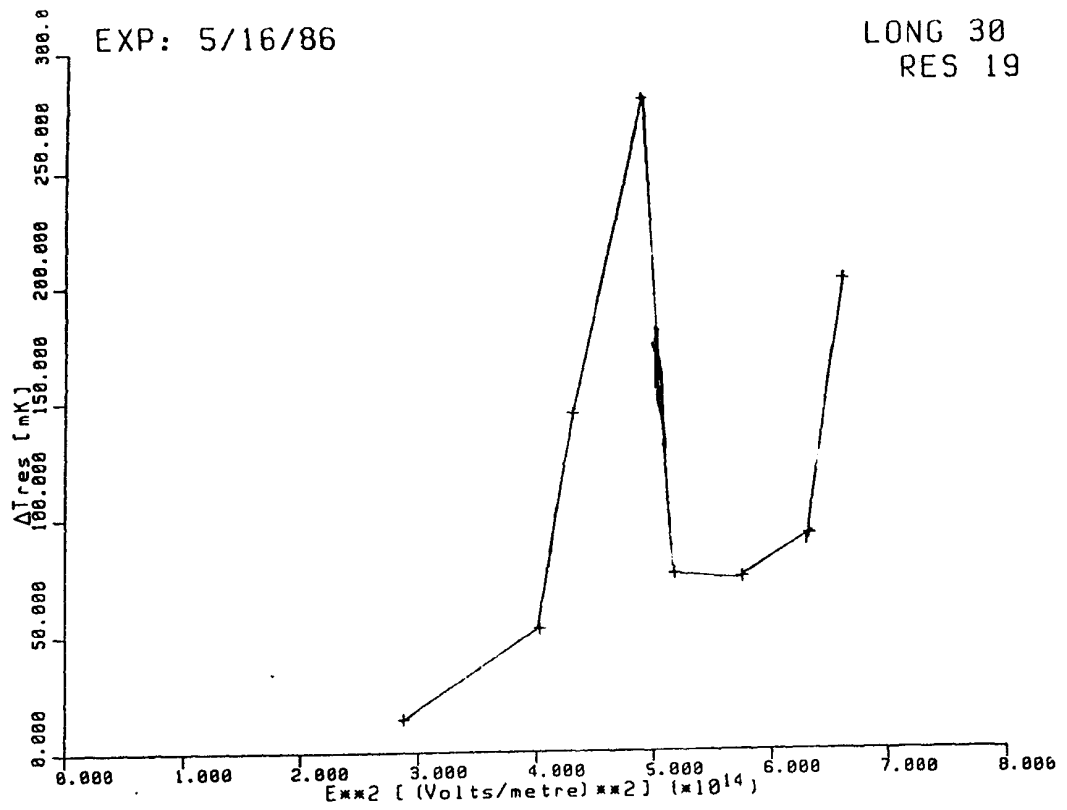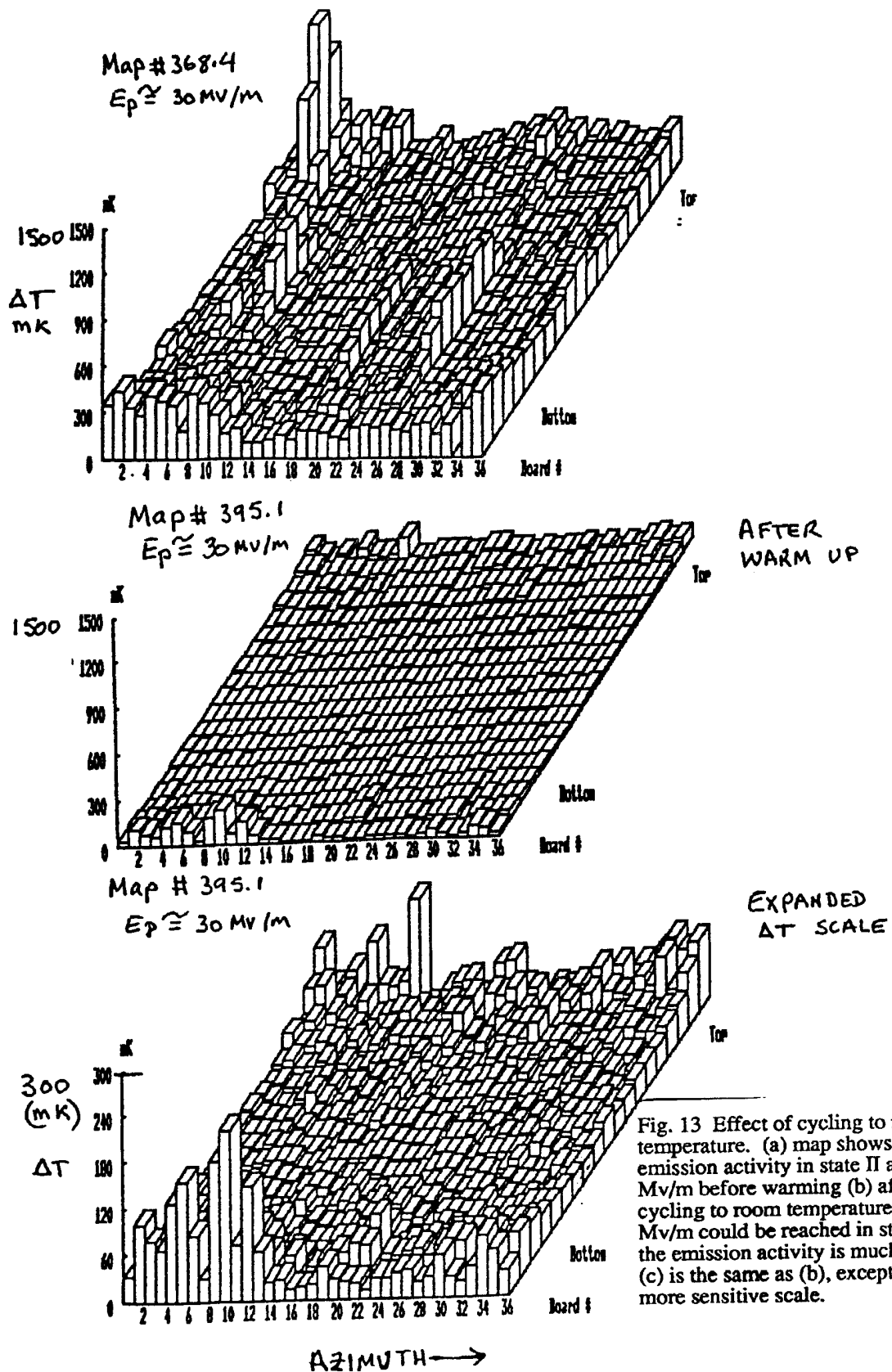
Fig. 12 Example of rf processing. Emission heating is abruptly reduced as the field level increases.

Fig. 13 Effect of cycling to room temperature. (a) map shows the emission activity in state II at 30 Mv/m before warming (b) after cycling to room temperature, 30 Mv/m could be reached in state I and the emission activity is much less. (c) is the same as (b), except on a more sensitive scale.

## Conclusions

Results with 3000 Mhz heat treated cavities have shown that overall FE loading is less after heat treatment and high fields can be reached more frequently. To improve our understanding of FE behavior in rf fields from cold surfaces, a high speed, superfluid He, thermometer based diagnostic system has been completed. A study of the behavior of FE in heat treated cavities has been started for 1500 Mhz cavities using the high speed/superfluid He thermometry diagnostic system. Heat treatments at 1100 and 1200 C have been tried and in both cases FE loading has been observed, including switching of emitters to a high emissive state. Surface Electric field values of 34 and 31 Mv/m could be reached, limited by heavy FE in state II. Comparison of T-maps between heat treated and chemically prepared surfaces at comparable field levels show that FE loading is reduced after heat treatment, but to reach higher fields than with chemically prepared surfaces, He processing was still necessary.

Our studies indicate that condensed gases play an important role in FE, so that it would be a worthwhile attempt to look for comparable phenomena in dc FE studies. We have also established that a Nb surface which can withstand a field of 30 Mv/m does not degrade on exposure to dust-free air, so that this avenue is not a rich source of emitters. We must look elsewhere for the sources of our regular field emitters.

For the future we plan to continue heat treatment at higher temperatures. We also plan controlled exposure of a high field cavity surface to clean methanol and clean water to determine if either of these are rich sources of emitters.

## REFERENCES

[1] H. Padamsee, "Status and Issues of Superconducting RF Technology", Proceedings of the 1987 Particle Accelerator Conference, Washington D.C. (1987)

[2] K. Shepard, Proc. of the 2nd Workshop on RF-Superconductivity, CERN, Ed. H. Lengeler, p 9, (1984)

[3] G. Mueller & H. Padamsee, "High Temperature Annealing of Superconducting Cavities Fabricated from High Purity Nb", Proceedings of the 1987 Particle Accelerator Conference, Washington D.C. (1987)

[4] Ph. Niedermann, this conference

[5] M. Tigner and H. Padamsee, Proc. of the 1982 Summer School on High Energy Particle Accelerators, 801, AIP Conf. Proc. No. 105 (1983)

[6] W. Weingarten, Proc. of the 2nd Workshop on RF-Superconductivity, CERN, Ed. H. Lengeler, p 30 (1984)

[7] H. Padamsee, C. Reece, R. Noer, W. Hartung, E. Frick, and R. Kahn, " Field Emission Studies in Superconducting Cavities", Proceedings of the 1987 Particle Accelerator Conference, Washington D.C. (1987)

[8] G. Mueller, Proc. of the 2nd Workshop on RF-Superconductivity, CERN, Ed. H. Lengeler, p 377 (1984)

[9] P. Kneisel, G. Mueller, and C. Reece, "Investigation of the Surface Resistance of Superconducting Nb Using Thermometry in Superfluid He", Proc. of the 1986 Applied Superconductivity Conference, Baltimore, Md (1986)

[10] G. Mueller, U. of Wuppertal, priv. communication

[11] H. A. Schwettman et. al, J. Appl. Physics, 45, 914(1975)

SRF87C03

## ACKNOWLEDGEMENTS

SRF87C03

SRF87C03